

# GALAXY LIGHT CONCENTRATION. I. INDEX STABILITY AND THE CONNECTION WITH GALAXY STRUCTURE, DYNAMICS, AND SUPERMASSIVE BLACKHOLES

Alister W. Graham, I. Trujillo, N. Caon

*Instituto de Astrofísica de Canarias, La Laguna, E-38200, Tenerife, Spain*

agraham@ll.iac.es, itc@ll.iac.es, ncaon@ll.iac.es

## ABSTRACT

We explore the stability of different galaxy light concentration indices as a function of the outermost observed galaxy radius. With a series of analytical light-profile models, we show mathematically how varying the radial extent to which one measures a galaxy’s light can strongly affect the derived galaxy concentration. The “mean concentration index”, often used for parametrizing high-redshift galaxies, is shown to be horribly unstable, even when modelling one-component systems such as Elliptical, dwarf Elliptical, and pure exponential disk galaxies. The  $C_{31}$  concentration index performs considerably better but is also heavily dependent on the radial extent, and hence exposure depth, of any given galaxy. We show that the recently defined central concentration index is remarkably stable against changes to the outer radius and observational errors, and provides both a meaningful and reliable estimate of galaxy concentration. The Sérsic index  $n$  from the  $r^{1/n}$  models is shown to be monotonically related with the central concentration of light, giving the index  $n$  a second and perhaps more tangible meaning. With a sample of Elliptical and dwarf Elliptical galaxies we present correlations between the central light concentration and the global parameters: luminosity (Pearson’s  $r = -0.82$ ), effective radius ( $r = 0.67$ ), central surface brightness ( $r = -0.88$ ), and velocity dispersion ( $r = 0.80$ ). The more massive Elliptical galaxies are shown to be more centrally concentrated. We speculate that the physical mechanism behind the recently observed correlation between the central velocity dispersion (mass) of a galaxy and the mass of its central supermassive blackhole may be connected with the central galaxy concentration. That is, we hypothesize that it may not simply be the amount of mass in a galaxy, but rather how that mass is distributed, which controls the mass of the central blackhole.

*Subject headings:* black hole physics, galaxies: fundamental parameters, galaxies: kinematics and dynamics, galaxies: nuclei, galaxies: photometry, galaxies: structure

## 1. Introduction

Estimates to the central concentration of galaxy light for the parametrization of galaxies go back many decades (Morgan 1958, 1959, 1962; subsequently known as the Yerkes system). Fraser (1972) made this method of classification quantitative with the introduction of the concentration indices  $C_{21}$  and  $C_{32}$ , defined as the ratio of radii that contain 50% and 25%, and 75% and 50%, of the total (asymptotic) galaxy luminosity. de Vaucouleurs (1977) expanded on this with the in-

troductioin of the more commonly used  $C_{31}$  index (see, for e.g., Kent 1985; Gavazzi, Garilli, & Boselli 1990; Moriondo et al. 1999).

Okamura, Kodaira, & Watanabe (1984) explored other fractional ratios and also introduced what they called the “mean concentration index”. This was a ratio of the luminous flux enclosed by two different radii rather than a ratio of radii (see section 2.2). Using an outer isophotal level of 26  $V$ -mag arcsec<sup>-2</sup>, Okamura et al. described how these indices are dependent on the intrinsic (or

mean) surface brightness of the individual galaxies. At least for Elliptical galaxies, or rather, one-component galaxies or bulges – which is what we wish to explore here – this can be directly translated into a dependency on the number of effective radii one samples. It is desirable to perform this translation because one replaces a dependency on two quantities, namely, the intrinsic surface brightness of each galaxy and the faintest surface brightness level observed, with one quantity (i.e. the number of scale-lengths or effective radii observed). It is this dependency which we wish to explore. Ideally, one would like to have a concentration index which is as independent as possible on this quantity (which is dependent on, amongst other things, the observational exposure details).

We use the Sérsic (1968)  $r^{1/n}$  law as a model-dependent way to illustrate the various concentration indices presented in Section 2. (The concentration indices, however, can be measured independently of this, and any, model.) All the concentration indices are dependent in some way on the extent to which the galaxy radial profile is sampled, and this dependency is revealed in Section 3. Truncating analytical light-profile models, we perform a comparative study of three different concentration indices. Additionally, using a range of observed Elliptical galaxy profiles obtained from deep exposures, we again explore the stability of the concentration indices.

In Section 4 we investigate the relationship between the galaxy light concentration and the other physical galaxy properties such as: luminosity, effective radius, central surface brightness, and velocity dispersion. Under the assumption that Elliptical galaxies are homologous systems, that is, assuming they all obey the  $r^{1/4}$  law, the concentration index of every Elliptical galaxy should be the same. However, research over the last decade has shown that Elliptical galaxies are not homologous and we present, in some cases, the first ever correlations between galaxy concentration and the global properties of Elliptical and dwarf Elliptical galaxies.

## 2. Concentration indices

We use the Sérsic  $r^{1/n}$  law as a mathematical means to illustrate the various concentration indices. The  $r^{1/n}$  luminosity-profile model has

been shown to provide a good representation to the distribution of light in both Elliptical galaxies (including the dwarf Ellipticals) and the bulges of Spiral galaxies (Caon, Capaccioli, & D’Onofrio 1993; D’Onofrio, Capaccioli, & Caon 1994; Young & Currie 1994; Andredakis, Peletier, & Balcells 1995), and is also appropriate for describing a Spiral galaxy’s disk. Although it’s appearance in the literature is becoming more frequent, we summarize it’s form below and introduce the parameters we will subsequently use throughout the paper.

The de Vaucouleurs (1948, 1959)  $r^{1/4}$  radial intensity profile  $I(r)$  was generalized by Sérsic (1968) to give the  $r^{1/n}$  law where

$$I(r) = I(0) \exp^{-b_n(r/r_e)^{1/n}}. \quad (1)$$

$I(0)$  is the central intensity and  $r_e$  the effective radius enclosing half of the flux from the model light profile. The quantity  $b_n$  is a function of the shape parameter  $n$  – which defines the global curvature in the luminosity profile – and is obtained from solving the expression  $\Gamma(2n) = 2\gamma(2n, b_n)$ , where  $\Gamma(a)$  and  $\gamma(a, x)$  are respectively the gamma function and the incomplete gamma function. The total luminosity,  $L_T$ , associated with an  $r^{1/n}$  profile that extends to infinity can be written as

$$L_T = I(0)r_{e,\text{mod}}^2 \frac{2\pi n}{b_n^{2n}} \Gamma(2n), \quad (2)$$

where  $r_{e,\text{mod}}$  is the effective half-light radius of the model. For elliptical (that is, non-spherical) galaxies,  $r_{e,\text{mod}}^2 = r_{e,\text{maj}}^2(1 - \epsilon)$ , where  $\epsilon$  is the ellipticity of the galaxy and  $r_{e,\text{maj}}$  is the major-axis half-light radius. The outer radius to which one (reliably) measures a galaxy is of course a function of exposure time, telescope aperture, etc. Denoting this outer finite (or final) radius as  $r_{\text{fin}}$ , the luminosity enclosed by this radius is

$$L(r_{\text{fin}}) = I(0)r_{e,\text{mod}}^2 \frac{2\pi n}{b_n^{2n}} \gamma\left(2n, b_n \left(\frac{r_{\text{fin}}}{r_{e,\text{mod}}}\right)^{1/n}\right). \quad (3)$$

Having introduced a model which can be used to represent the observed range of structural profile shapes in bulges, we can now proceed to describe the degree of concentration of light in these systems. The following definitions for the various concentration indices can all be applied without reference to the above (or any) light-profile model;

but it is of course insightful to use a parametrized model. We give below definitions or procedures to obtain the various concentration indices as a function of the outermost observed radius.

### 2.1. The concentration index $C_{31}$

Due to the popular use of  $C_{31}$  over  $C_{32}$  and  $C_{21}$ , we will focus on this particular concentration index related to the ratio of radii. The  $C_{31}$  index can either be obtained directly from the image, or using equation 2 and 3 when the observed luminosity profile is well fitted with an  $r^{1/n}$  model. Because light-profile models can first be convolved with the relevant point spread function before fitting to an observed profile, the latter approach has the strong advantage that corrections for seeing are already taken into account. Dividing equation 3 by equation 2 gives the fractional luminosity, denoted here by  $x$ , contained within the outermost observed radius  $r_{\text{fin}}$ . One then solves the ratio of equation 3 and equation 2 for the (new) values of  $r_{\text{fin}}/r_{e,\text{mod}}$  that give a fractional luminosity of  $0.75x$  and  $0.25x$ . The results of doing this are shown in Section 3.

### 2.2. The mean concentration index

The fundamental parameter in the classification system of Abraham et al. (1994) is basically the concentration index defined by Okamura et al. (1984) and Doi et al. (1993). It is a luminosity ratio between the flux enclosed by some inner radii and the outer-most radii, and has been parametrized in Abraham et al. (1994) such that

$$C(\alpha) = \frac{\sum_{i,j \in E(\alpha)} I_{ij}}{\sum_{i,j \in E(1)} I_{ij}}. \quad (4)$$

Here,  $I_{ij}$  represents the intensity in the pixel  $(i, j)$ , and  $E(\alpha)$  denotes some inner radius which is  $\alpha$  ( $0 < \alpha < 1$ ) times the outer radius which has been normalized to 1. Following Doi et al. (1993) Abraham et al. (1994) used a value of 0.3 for  $\alpha$ . In what follows in Section 3, we will use a value of  $\alpha = 1/3$ .

Trujillo et al. (2001b) noted that as the exposure depth increases and the outer radius therefore increases, this definition of light concentration loses its significance and tends to a value of 1 for all galaxies. For the Sérsic models, this concentration index can be written as a function of the

outer radius  $r_{\text{fin}}$  such that

$$C(\alpha) = \frac{\gamma \left[ 2n, b_n \left( \alpha \frac{r_{\text{fin}}}{r_{e,\text{mod}}} \right)^{1/n} \right]}{\gamma \left[ 2n, b_n \left( \frac{r_{\text{fin}}}{r_{e,\text{mod}}} \right)^{1/n} \right]}. \quad (5)$$

### 2.3. A new concentration index

We describe here a ‘third galaxy concentration’ (TGC) index defined in Trujillo et al. (2001b) as

$$TGC(\alpha) = \frac{\sum_{i,j \in E(\alpha r_e)} I_{ij}}{\sum_{i,j \in E(r_e)} I_{ij}}. \quad (6)$$

Here,  $E(r_e)$  means the isophote which encloses half of the total light of the galaxy<sup>1</sup>, and  $E(\alpha r_e)$  is the isophote at a radius  $\alpha$  ( $0 < \alpha < 1$ ) times  $r_e$ . Again, this is a flux ratio. For a Sérsic profile which extends to infinity,

$$TGC(\alpha) = \frac{\gamma(2n, b_n \alpha^{1/n})}{\gamma(2n, b_n)}. \quad (7)$$

For a range of different values of  $\alpha$ , this concentration index is shown in Figure 1 to increase monotonically with the value of  $n$ , revealing a relation between the central galaxy concentration of light and the global galaxy structure as defined by the shape parameter  $n$  (see Trujillo et al. 2001b). That is, the shape parameter  $n$  can be thought of as more than just a parameter that describes the curvature of the light profile, but has the additional physical meaning that it describes the degree of central concentration of at least luminous matter in Elliptical galaxies and bulges. This relation between the central luminous concentration and the global structure of the galaxy can be made even more succinctly by deprojecting the various  $r^{1/n}$  profile models to obtain their spatial luminosity density profiles (Ciotti 1991) for different values of  $n$  (Figure 2). One can immediately see the increasingly dramatic rise in central density<sup>2</sup> with increasing  $n$ .

For larger values of  $\alpha$  (e.g.  $>0.5$ ) the TGC index loses its ability to clearly distinguish galaxies with different structural profile shapes (i.e. different  $n$ ).

<sup>1</sup>In practice,  $r_e$  is the observed half-light radius  $r_{e,\text{obs}}$  and not  $r_{e,\text{mod}}$ .

<sup>2</sup>For  $n > 1$  the central density is actually infinite, occurring at a singularity (Ciotti 1991).

Low values for  $\alpha$ , such as 0.2, provide a good range to the TGC index for different  $n$ , but in reality are not so practical (especially when dealing with high-redshift galaxies). We therefore propose to use  $\alpha = 1/3$  (keeping the 3:1 ratio of the previous concentration indices).

Equation 3 shows how reducing the outer observed radius  $r_{\text{fin}}$  of an  $r^{1/n}$  profile reduces the observed galaxy luminosity. This in turn reduces the observed effective half-light radius from  $r_{e,\text{mod}}$  to  $r_{e,\text{obs}}$  (see Trujillo et al. 2001b, their Figure 9). As a result, the TGC index depends on the outer radius in the following way

$$TGC(\alpha) = \frac{\gamma \left[ 2n, b_n \left( \alpha \frac{r_{e,\text{obs}}}{r_{e,\text{mod}}} \right)^{1/n} \right]}{\gamma \left[ 2n, b_n \left( \frac{r_{e,\text{obs}}}{r_{e,\text{mod}}} \right)^{1/n} \right]}. \quad (8)$$

where  $r_{e,\text{obs}}/r_{e,\text{mod}}$  must first be computed given  $r_{\text{fin}}/r_{e,\text{mod}}$  (Trujillo et al. 2001b, their section 5.2).

### 3. Stability Analysis of the various concentration indices

In Figure 3 we have shown how the above three concentration indices vary as the outer final radius is varied. One can see that the commonly used concentrations indices do not simply reveal the luminous structural concentration one hopes to measure but can be heavily biased by the radial extent used to compute them. Consequently, concentration indices derived for exactly the same galaxies observed with first a ‘shallow’ and then a ‘deep’ exposure will be different. Clearly the “mean concentration index” (Section 2.2) is unreliable by itself to provide any kind of meaningful galaxy classification. Okamura et al. (1984) recognized this short-coming and, despite their hope to define a single fundamental structural quantity, had to resort to the introduction of an additional parameter, namely, the mean surface brightness of each galaxy. Even then they still had to acknowledge that the range of different global profile shapes (due also to the different bulge/disk combinations which galaxies possess) introduced additional scatter which left the previous two parameters still unable to provide an accurate classification of galaxy types along the morphological sequence (their Figure 3). They were however able to accurately (85%) classify galaxies as either

early-type (E-S0/a) or late-type (Sb-Im). This broad categorical restriction was confirmed by Doi et al. (1992), Doi, Fukugita, & Okamura (1993), and then again by Abraham et al. (1994) who explicitly dealt with ellipticity and extended the formalism to the study of small and faint images where individual pixel information is important. Doi et al. (1993) also showed that the effects of seeing can result in one not even being able to distinguish between these two broad categories when a small number of scale-lengths are sampled. Most recently, Bershady, Jangren, & Conselice (2000)<sup>3</sup> have introduced a third parameter, namely color – which Hubble (1936) noted was correlated with morphological type – that has enabled them to separate galaxies into three classes: early, intermediate, and late-type.

While the “mean concentration index” in combination with other galaxy parameters may be able to broadly categorize galaxies, it should clearly not be used as a tracer of the concentration of the luminous matter in galaxies. Its value depends sensitively on the depth of the image, and is therefore not closely related to any underlying physical property of the galaxy. Even for the same galaxy cluster, where the exposure details are the same, the situation is a mess. Figure 3 reveals that this index cannot even distinguish between a pure exponential disk (for e.g. an Sd galaxy) observed to three effective radii and a giant  $r^{1/4}$  elliptical galaxy observed to one effective radii.

The original concentration index defined as the ratio between radii enclosing different fractions (or quartiles) of the total galaxy luminosity (Fraser 1972; de Vaucouleurs & Aguero 1973; Fraser 1977; de Vaucouleurs 1977) is significantly more stable than the “mean concentration index”. This is because this index is less affected by where the galaxy profiles are taken to terminate. Although, it should be noted that this index is noticeably less well behaved when one removes the logarithm used in Figure 3. On the other hand, the TGC index appears to be very stable.

In order to compare the  $C_{31}$  index with the TGC index, we have plotted in Figure 4 the radii at which the two indices get within 10% of their

<sup>3</sup>Following Kent (1985), Bershady et al. (2000) used a ratio of radii for their concentration index  $C$ , such that  $C = 5 \log[r(80\%)/r(20\%)]$ .

asymptotic value, which occurs at an infinite radial extent. One can see that the TGC index acquires this level at a reasonable number of effective radii. The  $C_{31}$  index performs significantly worse. We therefore conclude that of the various concentration indices, the “mean concentration index” should not be used for the study of one-component systems (i.e. Elliptical galaxies, dwarf Elliptical galaxies, Spiral galaxy bulges, pure exponential disks). It’s application to two-component systems may be even less appropriate and will be studied in a forth-coming paper. The TGC index should be used in preference to the  $C_{31}$  index. The relative independence of the TGC index on the observed radial extent, and therefore on the individual intrinsic galaxy surface brightness and exposure details, may mean that this single parameter can be used on its own to quantify, at least one-component systems, without the need to obtain and calibrate surface brightness levels and colors; that is, even non-photometric data could be analyzed.

### 3.1. Tests with observed galaxy profiles

In the above section we have analyzed the stability of the various concentration indices against truncations in the radial extent of model Sérsic light-profiles. We now perform one of what is no doubt many possible tests which has no dependency on the Sérsic model and uses real galaxy profile data containing noise, sky-subtraction errors, and possible deviations from perfect  $r^{1/n}$  models.

In practice, to determine the total galaxy light attempts are made to account for the fraction of light which may reside outside the last measured isophote. In order to do this, the growth curve is normally extrapolated by one of a variety of techniques, such as a convenient mathematical function, or fitting some ad-hoc model, or even sometimes by eye. The extrapolation term, and the corresponding uncertainty, depend on a variety of factors, such as the shape of the light profile, the depth of the galaxian image, the accuracy of the sky-background subtraction, the particular way the extrapolation is computed, and so on. For this reason, it is of interest to compare (in a model-independent way) the measured concentration indices using observed profiles, and to check which index is least sensitive (i.e. more robust) to the

above potential sources of error in estimating the total galaxy light. The “mean concentration index” will not be computed here as it has already been shown to be a poor estimator of concentration, equal to 1 for any profile measured to a large radial extent.

We have analyzed the Virgo galaxy profiles presented in Caon et al. (1993, 1994) through the following experiment:

1. The galaxy growth curve was computed, out to the outermost measured radius, using the observed major-axis light profile and the ellipticity and position angle profiles. The total  $B$ -band magnitude was derived by extrapolating the growth curve to infinity (see the above two references) to give  $m_B$ .
2. Next, a variable magnitude  $\Delta m$  was added to  $m_B$  to give  $m_{\text{tot}}$ . Negative values of  $\Delta m$  correspond to changes in the magnitude due to an overestimate of the total galaxy luminosity; positive values may represent truncations in the light profile, or represent magnitudes within some isophotal threshold (such as  $V_{26}$ ), or simply account for errors from the true total galaxy magnitude.
3. From the value of  $m_{\text{tot}}$  we then derived the effective half-light radius  $r_{\text{eff}}$  and computed the TGC index. We also derived  $r_{25}$  and  $r_{75}$ , the radii at which the enclosed luminosity is 25% and 75% of the total luminosity, and determined the value of  $C_{31}$ . Both concentration indices were derived independently of any profile model.
4. Steps 2 and 3 were repeated for  $\Delta m$  ranging from  $-0.2$  to  $0.4$ .

By plotting these model-independently derived TGC and  $C_{31}$  indices as a function of  $\Delta m$ , we were able to see how they reacted to uncertainties/changes/errors in the total galaxy magnitude.

For a given variation in galaxy profile shape, and therefore galaxy concentration,  $C_{31}$  may change its value by  $x\%$  while the TGC index changes its value by  $y\%$ , or vice-versa. Therefore the stability of different indices can not be compared in terms of their percentage changes, as different percentage changes may accurately reflect identical changes in galaxy structure. The

sensitivity of each index to measurement errors should therefore perhaps be viewed in the light of the implied changes in galaxy structure. Figure 5 shows the derived TGC and  $C_{31}$  indices plotted against  $\Delta m$  for a random sub-sample of galaxies possessing a range of Sérsic indices  $n$ . It clearly shows that the TGC index is more stable than  $C_{31}$  because, for the same change in  $\Delta m$ , the TGC index spans a smaller interval in  $\Delta n$ , that is, a smaller change in galaxy structure. In other words, if one used the model-independent derivations for the TGC and  $C_{31}$  indices as a way to estimate the true galaxy structure as represented by  $n$ , the TGC index would give a more stable estimate which is less prone to uncertainties in  $m_{tot}$  than the index  $C_{31}$  is.

The above point is dramatically illustrated in Figure 6 and Figure 7. Figure 6 shows the TGC index derived from the best fitting Sérsic model to the observed galaxy light profile and the TGC index derived directly from the light profile data itself, with no dependence on a  $r^{1/n}$  model. In the model-independent case, the estimated total galaxy magnitude was then increased and decreased by  $\Delta m=0.2$  mag (i.e. spanning a range of 0.4 mag) and the TGC index re-computed. The first thing one notes from Figure 6 is that the model-dependent and model-independent values agree reasonably well with each other. The second point, which receives emphasis when one simultaneously considers Figure 7, is that the range in values for the TGC index is quite well constrained when one varies the total galaxy flux by nearly some 50%. The  $C_{31}$  index does not behave anywhere near as well (Figure 7). It can be clearly seen to be far less stable to errors in the total galaxy flux than what the TGC index is.

#### 4. Correlations between galaxy concentration, structure, and dynamics

The concentration index, in its various guises, has been shown to correlate, albeit sometimes poorly, with galaxy morphological type; indeed, Doi et al. (1993) suggested it be used, together with the observed mean surface brightness, as a means to morphologically classify different galaxy types (see also Bershadsky et al. 2000 and references within). We show for the first time in the following subsections that the TGC index, at least for

the family of Elliptical galaxies, is strongly correlated with all the fundamental galaxy parameters. The concentration appears to not only reflect the general morphological structure, but is intimately related with the total luminosity, size, brightness, and central velocity dispersion of a galaxy.

One may ask, “But isn’t the TGC index merely another way of expressing the exponent  $n$ ?” Or, is this central concentration index (a quantity which can be measured independently of any model or value of  $n$ ) a fundamental quantity which is intimately linked with the nature and evolution of Elliptical galaxies. What are the fundamental quantities which should be plotted against each other to gain insight into the nature of Elliptical galaxies? At this point we don’t know. We therefore show, for a sample of Elliptical galaxies, correlations between concentration and: luminosity, surface-brightness, scale-size. and velocity dispersion. What past correlations with  $n$  actually mean are somewhat vague. Only when you understand what the correlations mean are you able to say something about the physical behavior of galaxies. What we shall see below is that the larger, more luminous and massive galaxies are more centrally concentrated.

##### 4.1. Luminosity

The previous analysis, in particular Figure 1, reveals that the central luminous concentration in Elliptical galaxies, and also Spiral galaxy bulges, must be related to their global luminous structure. This is because the more luminous galaxies and bulges are known to possess larger values of  $n$  (Caon et al. 1993; Young & Currie 1994, 1995; Andredakis et al. 1995; Jerjen & Binggeli 1997; Graham 2001) and consequently they must also have higher central concentrations of light than the less luminous bulges. Figure 8 shows that this is indeed the case. Here, the TGC index has been plotted against the bulge luminosity from a sample of Virgo dwarf Elliptical galaxies (Jerjen, Binggeli, & Freeman 2000) and a sample of Virgo and Fornax early-type galaxies (Caon et al. 1993; D’Onofrio et al. 1994). The Pearson correlation coefficient between the TGC index and luminosity is  $-0.82$ . Given our new understanding of the relationship between the Sérsic index  $n$  and the central concentration of luminous mass, the correlation between total luminosity and concentration is perhaps not

surprising. It has, however, to the best of our knowledge, never been shown before for a sample of Elliptical galaxies. It can also be derived completely independent of any light-profile model (and hence value of  $n$ ), although here we have used the TGC index from the best-fitting Sérsic model because of the similarity seen in Figure 6 and because we do not have the images for the dwarf galaxy data set.

To calibrate the luminosity density profiles in Figure 2 requires some measure of the central intensity or central surface brightness  $\mu_0$  which is, for an  $r^{1/4}$  model, 7.67 mag brighter than the surface brightness  $\mu_e$  at one effective radius. Now, the Kormendy (1977) relation for Elliptical galaxies tells us that  $\mu_e \propto 3 \log r_e$ , and therefore<sup>4</sup> the magnitude  $M \propto -2 \log r_e$ . Thus, assuming  $r^{1/4}$  profiles, the more luminous galaxies should possess larger effective radii and *fainter* central intensities, which equivalently implies lower central luminosity densities.

It must be stressed that we are not referring to the behavior of the luminosity density of the core within the central  $\sim$ arcsecond as revealed with HST resolution (Rest et al. 2001, and references within), but to the properties derived from the global galaxy profile. Recent findings show that many Elliptical galaxies possess supermassive blackholes at their centers (Kormendy & Gebhardt 2001 and references within). Gravitational slingshots of stars which come to close to the central massive blackhole, or coalescing massive blackholes from the progenitors of a merger may, to varying degrees, evacuate the core of a bulge and thereby reduce the original inner light profile (Ebisuzaki, Makino, & Okamura 1991; Makino & Ebisuzaki 1996; Quinlan 1996; Quinlan & Hernquist 1997; Faber et al. 1997; Milosavljević & Merritt 2001). If mergers involve strong gaseous dissipation and central starbursts this may also modify the nuclear profile (Mihos & Hernquist 1994), as do adiabatic black hole growth models (van der Marel 1999a,b, 2001). In this paper we are, however, not talking about the very inner density of HST-resolved nuclear cusp slopes which may have been modified by the central blackhole, but are referring to the global galaxy structure as seen with ground based resolution.

<sup>4</sup>For an  $r^{1/4}$  law,  $m = \mu_e - 5 \log r_e - 3.388$ .

The estimated masses of the central blackholes in bulges have been shown to positively correlate with the total luminosity of the host galaxy (Kormendy 1993; Kormendy & Richstone 1995), which would imply, assuming  $r^{1/4}$  profiles, that their masses are greater for galaxies with lower central luminosity densities (again, we are not referring to the modified HST resolved cusps). Why it should be that galaxies which are globally more disperse have greater central blackhole masses must be explained if one is to assume that all Elliptical galaxies follow the  $r^{1/4}$  law. However, this problem is quickly dismissed when one realises that it is a somewhat artificial problem which was created from the simplification of galaxies through the assumption of  $r^{1/4}$  profiles. Not only do a range of light profile shapes exist, as do varying degrees of concentration, but the central (observed with ground-based telescopes) surface brightness of all but the brightest Elliptical galaxies actually brighten with increasing galaxy magnitude (Figure 9)<sup>5</sup> in contradiction to the prediction of the Kormendy relation when coupled with the assumption of  $r^{1/4}$  profiles. That is not to say that the Kormendy relation is wrong. Indeed, the brighter galaxy sample members in Figure 9 roughly follow the Kormendy relation, having a slope of  $\sim 3$  in the  $\mu_e - \log r_e$  plane (Figure 10). (Although, the smaller and fainter galaxies do not follow the Kormendy relation, but there is certainly no suggestion that  $\mu_e$  brightens with  $r_e$ .) Figure 9 reveals that the mass of the central supermassive blackholes are therefore positively correlated with the central luminosity density of the host galaxy as derived from the global luminosity profile, with the caveat that the very inner light profile cusps have likely been re-shaped by the central massive blackhole.

We wanted to be confident that the trend seen in Figure 9 could not be explained by the influence of atmospheric seeing on what might in fact be  $r^{1/4}$  law profiles which have smaller half-light radii the fainter the galaxy magnitudes are. To explore this we convolved a series of  $r^{1/4}$  profiles having a range of half-light radii from 5 to 50 arcsec with a Gaussian PSF having a FWHM of 2 arcsec, comparable to the worst seeing conditions under which

<sup>5</sup>There is some suggestion of a turn around at  $B_T < 10$  in Figure 9, evident amongst the brightest galaxy members in Figure 6c of Faber et al. 1997.

the central CCD data was obtained for the galaxy sample shown in Figure 9. We found that the average surface brightness within the inner circle of radius 1 arcsec was under-estimated by  $\sim 0.5$  mag arcsec $^{-2}$  when  $r_e=5''$  and by  $\sim 0.3$  mag arcsec $^{-2}$  when  $r_e=50''$ . These differences were of course even smaller when the values within the inner  $2''$  radius were considered, and the trend seen in Figure 9 did not vary noticeably when we used the observed data within the inner  $2''$ . The effects of seeing are therefore unable to resurrect the possibility that the trend seen in Figure 9 is compatible with all galaxies having  $r^{1/4}$  law profiles.

#### 4.2. Central surface brightness and effective radii

Khosroshahi, Wadadekar, & Kembhavi (2000) and Mollenhoff & Heidt (2000) have modelled the light profiles from a sample of spiral galaxies with a seeing-convolved  $r^{1/n}$  bulge and exponential disk model. The strongest correlation found between any of the structural parameters explored by these authors was between the central bulge surface brightness and the bulge shape parameter  $n$ . Khosroshahi et al. obtained a linear correlation coefficient  $r = -0.88$  at a significance level better than 99.99%, and Mollenhoff et al. obtained a value of  $r = -0.86$ . Positive correlations between  $n$  and  $r_e$  were also found by these authors. Thus, from Section 2, the central luminosity density of spiral galaxy bulges (as represented by  $\mu_0$ ) must be positively correlated with not only  $n$  but also with the bulge concentration of luminous matter. One may indeed ask which is the more fundamental connection.

We show in Figure 11 and Figure 12 the correlation between the TGC index and  $r_e$  and  $\mu_0$  for our sample of dwarf Elliptical and Elliptical galaxies. The behavior in Figure 11 is similar to that already known between  $n$  and  $r_e$  (e.g. Caon et al. 1993; Graham et al. 1996). The correlation coefficient is 0.67, and turns out to be the weakest correlation we find between concentration and any of the other galaxy parameters presented here.

In Trujillo et al. (2001b) we showed that the range of different galaxy structures which exists amongst the Elliptical population cannot be due to parameter coupling in the  $r^{1/n}$  models, and systematically varies with model-independent quantities such as effective half-light radius and lumi-

osity. We caution, however, that for large values of  $n$  the effects of seeing on the light profile can be substantial at small radii (Trujillo et al. 2001a). We also note that while the  $r^{1/n}$  profiles are good at describing the global profile shape, they can require modification at some small inner radii (Jaffe et al. 1994; Ferrarese et al. 1994; Lauer et al. 1995; Faber et al. 1997). The notably bright ( $\sim < 15$  mag arcsec $^{-2}$ ) central ( $r=0$ ) surface brightnesses expected from the very high values of  $n$  are perhaps also unlikely to be realised. Either the Sérsic model is no longer appropriate to describe the very inner profile, and/or the extremely high inner densities modify the actual profile. The presence of (and likely past infall of material into) a central supermassive BH is also likely to disturb the central cusp slope, as can mergers and other mechanisms (Makino & Ebisuzaki 1996; Faber et al. 1997; Quinlan & Hernquist 1997; Merritt & Quinlan 1998). We therefore note that Figure 12 (see also Jerjen & Binggeli 1997), showing the relation between the TGC index and the central galaxy surface brightness obtained from the best-fitting  $r^{1/n}$  model, should be regarded as somewhat preliminary and a more detailed investigation shall be forthcoming. Despite these words of caution, excluding those galaxies with values of  $n$  greater than 4, that is, removing those galaxies which may have overly bright central surface brightness estimates, still resulted in a correlation coefficient of  $-0.88$  between the central concentration and central surface brightness. (Using all of the galaxies gave a correlation coefficient  $r = -0.94$ .) We stress again that if all Elliptical galaxies followed the  $r^{1/4}$  law, then the concentration index would be the same for all galaxies, and no correlation would exist between concentration and any of the other galaxy parameters; this is similarly the case if all dwarf Elliptical galaxies and Spiral galaxy bulges were to possess the same universal profile.

#### 4.3. Velocity dispersion and mass

Combining the luminosity – central concentration relation (Figure 8) with the Faber-Jackson (1976) relation between luminosity and central velocity dispersion immediately implies that the central velocity dispersion and therefore mass – as far as the central velocity dispersion is a measure of the galaxy mass – must positively correlate with the galaxy concentration. Using the early-type

galaxies from Caon et al. (1993) and D’Onofrio et al. (1994) which have available central velocity dispersion measurements from Hypercat<sup>6</sup>, Figure 13 shows that the TGC index is strongly ( $r = 0.80$  for the Ellipticals) correlated with the velocity dispersion, even with the heterogeneous nature of the dynamical data. Excluding galaxies with central velocity dispersions less than  $100 \text{ km s}^{-1}$  did not change things appreciably, nor did using the central velocity dispersion catalog of McElroy (1995) where we found a value of  $r = 0.82$ . This is a fundamental result; together with the previous correlations it tells us that the more massive a galaxy is, the more centrally concentrated it must be. The virial theorem (and its observational counterpart the Fundamental Plane: Djorgovski & Davis 1987; Dressler et al. 1987) relates the luminosity, size, and velocity dispersion (kinetic energy) terms, but does not explain why greater mass should imply higher central concentration. Theories of gravitational collapse and galaxy formation must be able to explain this.

We speculate here that galaxy concentration may provide the physical mechanism for the observed connection between the stellar velocity dispersion (mass) of a bulge and the mass of its central supermassive BH (Merritt 2000; Ferrarese & Merritt 2000; Gebhardt et al. 2000; Merritt & Ferrarese 2001; Marconi et al. 2001; Sarzi et al. 2001). The exact process which explains the reason for the existence of this correlation is not yet known, although many theories have been proposed (Efsthathiou & Rees 1988; Haehnelt & Rees 1993; Ciotti & Ostriker 1997; 2001; Haiman & Loeb 1998; Silk & Rees 1998; Blandford 1999; Haehnelt & Kauffman 2000; Kauffman & Haehnelt 2000; Ostriker 2000; Adams, Graff, & Richstone 2001). Bigger galaxies with higher central concentration and stronger potential wells would naturally supply more fuel to their inner regions. This could take the form of more efficiently funneling gas to build the central accretion disks that likely feed the quasars we observe at high-redshift (Soltan 1982), perhaps leaving remnants such as the nuclear disks we observe today (Rest et al. 2001 and references within) which would now encircle the inactive heart of what was once a quasar.

---

<sup>6</sup>Hypercat can be reached at <http://www-obs.univ-lyon1.fr/hypercat/>.

It is not clear why simply having a higher velocity dispersion alone can be the fundamental physical mechanism for greater BH masses. On the one hand it does imply that more material (mass) is in the galaxy to build/feed a blackhole, but we saw in Section 4.1 that if all galaxies were described by the  $r^{1/4}$  law then galaxies with greater mass (higher velocity dispersion) would have *lower* central luminosity densities and be more disperse. This would require a low-density environment to either favor the formation of more massive blackholes or to be the product of their evolution. (Once again, we stress that we are not referring to the very inner nucleus as revealed with HST imaging.) We propose here that the presence of mass itself may not be the end of the story. Figure 13 shows that more massive galaxies are more centrally concentrated than less massive galaxies. We suggest that exactly how the galaxy mass is distributed/concentrated may be an important factor. This could be tested through a photometric campaign which measures the concentration in those galaxies with blackhole mass estimates, and determines the strength and scatter of the correlation between these two quantities. Although, Ferrarese & Merritt (2001) and Gebhardt et al. (2000) found that the intrinsic scatter in the BH mass – velocity dispersion diagram is small or negligible (i.e. consistent with the measurement errors alone) for those galaxies with most reliable blackhole mass measurements. This would then leave no room for improvement with a BH mass - galaxy concentration diagram, and would suggest that the former is indeed the more fundamental relation. This result may hold firm, although it will be of interest to see what happens when more BH mass estimates are obtained and refined on several fronts. Improvements will come with the use of non-axisymmetric dynamical models, improved knowledge of line broadening mechanisms (Barth et al. 2001), and addressing concerns that the dynamical effects of some blackholes may occur at resolutions lower than presently probed (Qian et al. 1995; de Zeeuw 2000). Additional corrections for the finite slit width of STIS on the HST (Maciejewski & Binney 2001) may also prove crucial, and significantly lower the current blackhole mass estimates.

## 5. Conclusions

We have explored the stability of several different galaxy light concentration indices as a function of galaxy exposure depth, or rather, the number of effective radii sampled. This analysis has been confined to one-component stellar systems such as normal Elliptical galaxies, dwarf Elliptical galaxies, Spiral galaxy bulges, and exponential disks. Our investigation reveals that the “mean concentration index”, often used for parametrizing faint and high-redshift galaxies, is a horrendously poor estimator of galaxy light concentration and its use for such a task on its own should be abandoned. To illustrate this claim, we have shown that this index is unable to distinguish between a giant  $r^{1/4}$  Elliptical galaxy measured to one effective radii and a pure exponential disk measured to three effective radii. The de Vaucouleurs  $C_{31}$  index performs notably better but is still heavily dependent on the outer galaxy radius one reaches. The central concentration index introduced in Trujillo et al. (2001b) is shown to be the more stable of the indices, changing in value (with increasing galaxy radius) by less than 10% once a few effective radii have been sampled, and is more robust against measurement errors.

Given that Elliptical galaxies and bulges are not homologous systems, they therefore possess a range of different (light) concentrations. The global profile shape, which can be parameterized by the value  $n$  from the Sérsic  $r^{1/n}$  law, is intimately connected with the degree of galaxy light (and mass) concentration. Which of these two quantities is the more fundamental is not clear; the latter quantity can however be measured directly from the image or light-profile, derived independently of any galaxy model. For a sample of dwarf Elliptical galaxies and normal Elliptical galaxies we have presented strong correlations between the central concentration index, as defined in this paper, and the global galaxy parameters: luminosity, effective radius, and central surface brightness. We also present the first ever correlation between galaxy concentration and velocity dispersion for a sample of Elliptical galaxies, showing that the more massive galaxies are more centrally concentrated; this should provide a valuable clue into the physics of gravitational collapse and galaxy formation. Lastly, we speculate and provide a means to

test that the central concentration of at least luminous matter in Elliptical galaxies, that is, how this matter is distributed, may be an important quantity regarding the formation of supermassive BHs.

We are happy to thank Helmut Jerjen for providing us with the dwarf Elliptical data used in Figure 8-12. We also wish to acknowledge and thank the anonymous referee for their suggestions and comments which helped to improve this paper.

## REFERENCES

- Abraham, R.G., Valdes, F., Yee, H.K.C., & van den Bergh, S. 1994, *ApJ*, 432, 75
- Andredakis, Y.C., Peletier, R.F., & Balcells, M. 1995, *MNRAS*, 275, 874
- Barth, A.J., Sarzi, M., Rix, H.-W., Ho, L.C., Filippenko, A.V., & Sargent, W.L.W. 2001, *ApJ*, in press (astro-ph/0012213)
- Bershady, M.A., Jangren, A., & Conselice, C.J. 2000, *AJ*, 119, 2645
- Blandford, R.D. 1999, in *ASP Conf. Ser.* 182, *Galaxy Dynamics*, ed. D. Merritt, J.A. Sellwood, & M. Valluri (San Francisco: ASP), 87
- Caon, N., Capaccioli, M., & D’Onofrio, M. 1993, *MNRAS*, 265, 1013
- Caon, N., Capaccioli, M., & D’Onofrio, M. 1994, *A&AS*, 106, 199
- Caon, N., Capaccioli, M., & Rampazzo, R. 1990, *A&AS*, 86, 429
- Ciotti, L. 1991, *A&A*, 249, 99
- Ciotti, L., & Ostriker, J.P. 1997, *ApJ*, 487, L105
- Ciotti, L., & Ostriker, J.P. 2001, *ApJ*, 551, 131
- de Vaucouleurs, G. 1948, *Ann. d’Astrophys.*, 11, 247
- de Vaucouleurs, G. 1959, *Hdb. d. Physik*, 53, 311
- de Vaucouleurs, G. 1977, in *Evolution of Galaxies and Stellar populations*, eds. R. Larson & B. Tinsley (New Haven: Yale University Observatory) p.43
- de Vaucouleurs, G., & Aguero, E. 1973, *PASP*, 85, 150
- Djorgovski, S., & Davis, M. 1987, *ApJ*, 313, 59

- Doi, M., Kashikawa, N., Okamura S., Tarusawa, K., Fukugita, M., Sekiguchi, M., & Iwashita, H. 1992, in *Digitised Optical Sky Surveys*, Kluwer, Dordrecht, p.199
- Doi, M., Fukugita, M., & Okamura, S. 1993, *MNRAS*, 264, 832
- D’Onofrio, M., Capaccioli, M., & Caon, N. 1994, *MNRAS*, 271, 523
- Dressler, A., Lynden-Bell, D., Burstein, D., Davies, R.L., Faber, S.M., Terlevich, R.J., & Wegner, G. 1987, *ApJ*, 313, 42
- Ebisuzaki, T., Makino, J., & Okamura, S.K. 1991, *Nature*, 354, 212
- Efstathiou, G., & Rees, M.J. 1988, *MNRAS*, 230, 5p
- Faber, S.M., & Jackson, R.E. 1976, *ApJ*, 204, 668
- Faber, S.M., et al. 1997, *AJ*, 114, 1771
- Ferrarese, L., & Merritt, D. 2000, *ApJ*, 539, L9
- Ferrarese, L., van den Bosch, F.C., Jaffe, W., Ford, H.C., & O’Connell, R.W. 1994, *AJ*, 108, 1598
- Fraser, C.W. 1972, *The Observatory*, 92, 51
- Fraser, C.W. 1977, *A&AS*, 29, 161
- Gavazzi, G., Garilli, B., & Boselli, A. 1990, *A&AS*, 83, 399
- Gebhardt, K., et al. 2000, *ApJ*, 539, L13
- Graham, A.W., Lauer, T.R., Colless, M.M., & Postman, M. 1996, *ApJ*, 465, 534
- Graham, A.W. 2001, *AJ*, 121, 820
- Haehnelt, M.G., & Kauffmann, G. 2000, *MNRAS*, 318, L35
- Haehnelt, M.G., & Rees, M.J. 1993, *MNRAS*, 263, 168
- Haiman, Z., & Loeb, A. 1998, *ApJ*, 503, 505
- Hubble, E. 1936, *The Realm of the Nebulae* (New Haven: Yale Univ. Press)
- Jaffe, W., Ford, H.C., Ferrarese, L., van den Bosch, F.C., & O’Connell, R.W. 1994, *AJ*, 108, 1567
- Jerjen, H., & Binggeli, B. 1997, in *The Nature of Elliptical Galaxies; The Second Stromlo Symposium*, ASP Conf. Ser., 116, 239
- Jerjen, H., Binggeli, B., & Freeman, K.C. 2000, *AJ*, 119, 593
- Kauffmann, G., & Haehnelt, M. 2000, *MNRAS*, 311, 576
- Kent, S. 1985, *ApJS*, 59, 115
- Kormendy, J. 1977, *ApJ*, 218, 333
- Kormendy, J. 1993, in *The Nearest Active Galaxies*, ed. J. Beckman, L. Colina, & H. Netzer (Madrid: CSIC), 197
- Kormendy, J., & Richstone, D. 1995, *ARA&A*, 33, 581
- Kormendy, J., & Gebhardt, K. 2001, in *The 20th Texas Symposium on Relativistic Astrophysics*, ed. H. Martel, & J.C. Wheeler, AIP, in press
- Khosroshahi, H.G., Wadadekar, Y., & Kembhavi, A. 2000, *ApJ*, 533, 162
- Lauer, T.R., et al. 1995, *AJ*, 110, 2622
- Makino, J., & Ebisuzaki, T. 1996, *ApJ*, 465, 527
- Maciejewski, W., & Binney, J. 2001, *MNRAS*, 323, 831
- Marconi, A., et al. 2001, *IAU Symposium 205 “Galaxies and their Constituents at the Highest Angular Resolutions”*, R. Schilizzi, S. Vogel, F. Paresce, M. Elvis eds, ASP Conf. Ser
- McElroy, D.B. 1995, *ApJS*, 100, 105
- Merritt, D. 2000, in *ASP Conf. Ser. 197, Dynamics of Galaxies: From the Early Universe to the Present*, ed. F. Combes, G.A. Mamom, & V. Charmandaris (San Francisco: ASP), 221
- Merritt, D., & Ferrarese, L. 2001, *ApJ*, 547, 140
- Merritt, D., & Quinlan, G.D. 1998, *ApJ*, 498, 625
- Mihos, J.C., & Hernquist, L. 1994, *ApJL*, 437, L47
- Milosavljević, M., & Merritt, D. 2001, *ApJ*, submitted (astro-ph/0103350)
- Mollenhoff, C., & Heidt, J. 2001, *A&A*, submitted
- Morgan, W.W. 1958, *PASP*, 70, 364
- Morgan, W.W. 1959, *PASP*, 71, 394
- Morgan, W.W. 1962, *ApJ*, 135, 1
- Moriondo, G., et al. 1999, *A&AS*, 137, 101
- Okamura, S., Kodaira, K., & Watanabe, M. 1984, *ApJ*, 280, 7
- Ostriker, J.P. 2000, *Phys. Rev. Lett.*, 84, 5258
- Qian, E.E., de Zeeuw, P.T., van der Marel, R.P., Hunter, C. 1995, *MNRAS*, 274, 602

- Quinlan, G.D. 1996, *New Astronomy*, 1, 35
- Quinlan, G.D., & Hernquist, L. 1997, *New Astronomy*, 2, 533
- Rest, A., van den Bosch, F.C., Jaffe, W., Tran, H., Tsvetanoy, Z., Ford, H.C., Davies, J., & Schafer, J. 2001, *AJ*, in press (astro-ph/0102286)
- Sarzi, M., Rix, H.-W., Shields, J.C., Rudnick, G., Ho, L.C., McIntosh, D.H., Filippenko, A.V., & Sargent, W.L.W. 2001, 550, 65
- Sérsic, J.-L. 1968, *Atlas de Galaxias Australes* (Cordoba: Observatorio Astronomico)
- Silk, J., & Rees, M.J. 1998, *A&A*, 331, L1
- Solton, A. 1982, *MNRAS*, 200, 115
- Trujillo, I., Aguerri, J.A.L., Cepa, J., & Gutiérrez, C.M. 2001a, *MNRAS*, 321, 269
- Trujillo, I., Graham, A.W., & Caon, N. 2001b, *MNRAS*, in press
- van der Marel, R.P. 1999a, *AJ*, 117, 744
- van der Marel, R.P. 1999b, *IAU Symp. 186: Galaxy Interactions at Low and High Redshift*, eds. J.E. Barnes, D.B. Sanders, Kluwer: Dordrecht, 186, 333
- van der Marel, R.P. 2001, *IAU Symposium 205 "Galaxies and their Constituents at the Highest Angular Resolutions"*, R. Schilizzi, S. Vogel, F. Paresce, M. Elvis eds, ASP Conf. Ser
- Young C.K., Currie M.J. 1994, *MNRAS*, 268, L11
- Young C.K., Currie M.J. 1995, *MNRAS*, 273, 1141
- de Zeeuw, T. 2000, In *ESO Conference on Black Holes in Binaries and Galactic Nuclei*, eds. L. Kaper and E.P.J. van den Heuvel

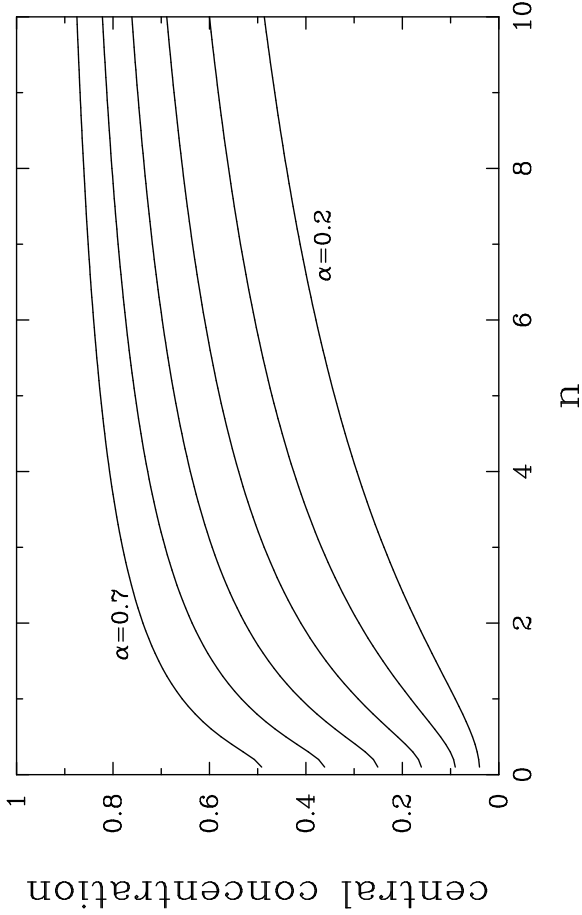


Fig. 1.— The central galaxy concentration index as defined in equation 6 and equation 7 is shown as a function of the Sérsic shape parameter  $n$ , for different values of  $\alpha$ . (Extension of Figure 3 from Trujillo et al. (2001b) who plotted values of  $\alpha$  equal to 0.3 and 0.5.)

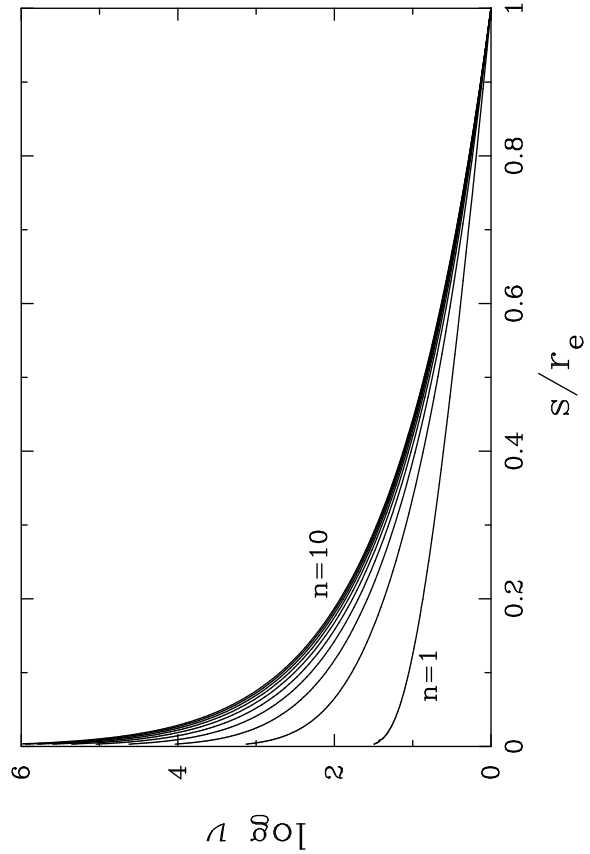


Fig. 2.— The deprojected (spatial) luminosity-density profiles for a range of Sérsic  $r^{1/n}$  models are shown as a function of the deprojected radius  $s$ , normalized at  $1 r_e$  from the projected  $r^{1/n}$  model. The increased central concentration of these models with  $n$  is strong and obvious.

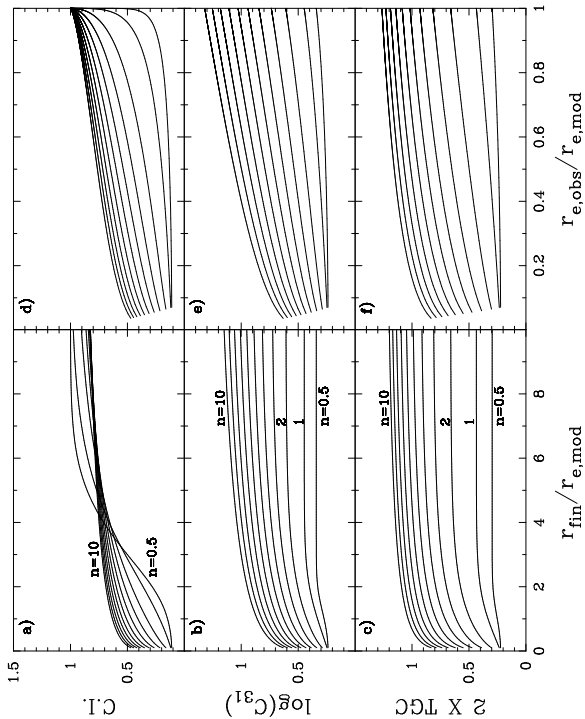


Fig. 3.— Various concentration indices have been plotted, for different galaxy profile shapes  $n$ , as a function of the outer radius  $r_{\text{fin}}$  used to compute each index (see text for details). Panel a) presents the concentration index as defined by Abraham et al. (1994). Panel b) presents the logarithm of the concentration index defined by de Vaucouleurs (1977). Panel c) presents the concentration index defined by Trujillo et al. (2001b). Panel d) to f) show the various indices as a function of the observed half-light radius, which changes with  $r_{\text{fin}}$ . The value of  $\alpha$  used to compute  $C_{31}$  and  $TGC$  has been set to  $1/3$ . The  $TGC$  index is clearly the most stable of the three, while the index in panel a) is horrendously unstable.

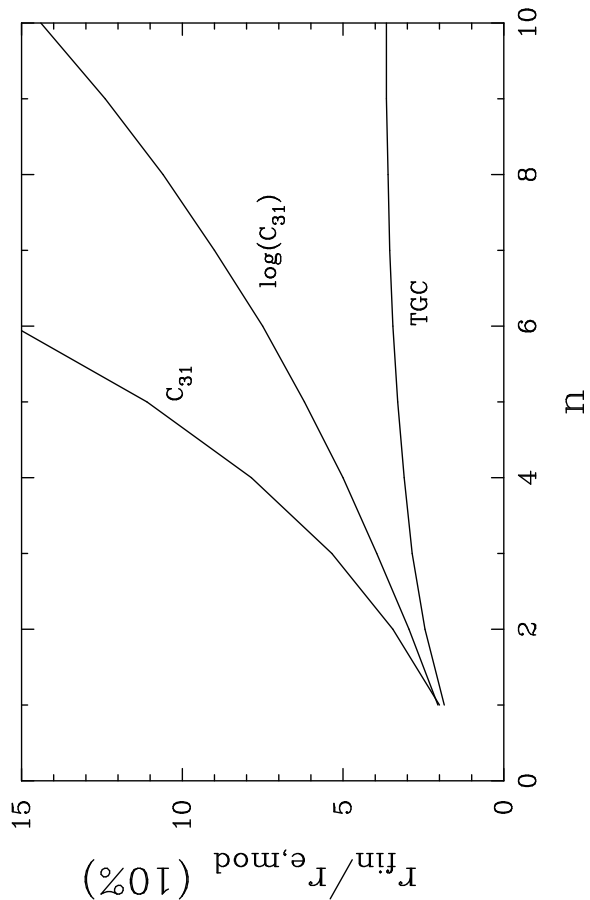


Fig. 4.— Stability analysis of the the  $C_{31}$  concentration index and the  $TGC$  index. The radius  $r_{\text{fin}}$  (normalized by the effective radius  $r_{e,\text{mod}}$  of each  $r^{1/n}$  model) where the concentration indices get within 10% of their maximum value (which occurs at an infinite radial extent) is shown as a function of  $n$ . The  $TGC$  index is clearly more stable with radius, and hence exposure depth, than the  $C_{31}$  index.

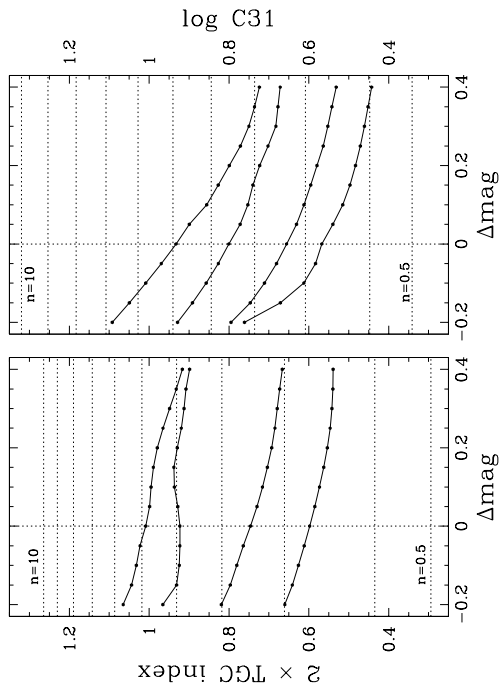


Fig. 5.— TGC and  $C_{31}$  indices (computed independently of any Sérsic  $r^{1/n}$  model) for a sample of real galaxy profiles spanning a range of structural shapes (i.e.  $n$ ). The light-profile data was taken from Caon et al. (1990) and (1994) for NGC 4623, NGC 1379, NGC 4636, and NGC 4365, in order of increasing galaxy light concentration. The influence on the concentration indices by supplementing the observed galaxy magnitude within some outer radius with  $\Delta m$  is revealed (see text for details). The term  $\Delta m$  can represent the magnitude beyond the outer radius which was missed, or represent truncations to an inner isophotal level, or one of a number of sources of observational error. Dotted horizontal lines mark the values of the TGC and  $C_{31}$  indices corresponding to infinite Sérsic models with  $n = 0.5, 1, 2, \dots, 10$ .

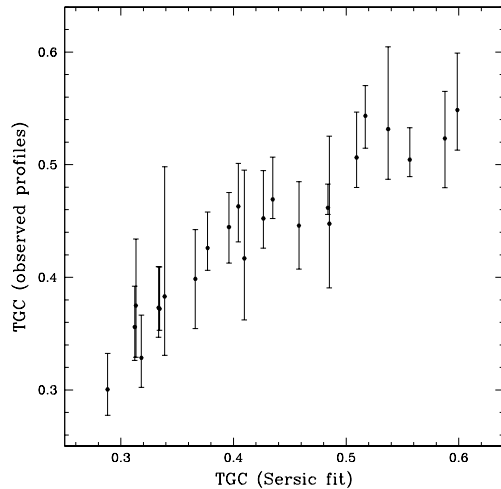


Fig. 6.— The stability of the TGC index has been explored with real galaxy data by deriving its (model-independent) value when an error of  $\pm 0.2$  mag is added to the (model-independent) estimated total galaxy magnitude. The  $x$ -axis is the TGC index derived from the best-fitting Sérsic model. Only galaxies with major-axis fits which were marked as ‘Good’ (that is, not those whose quality was marked as ‘Fair’ or ‘Poor’) from Table 2 of Caon et al. (1993) have been used.

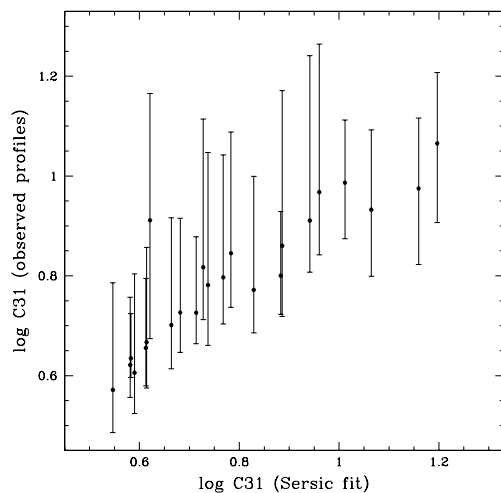


Fig. 7.— Same as Figure 6 but for the  $C_{31}$  index.

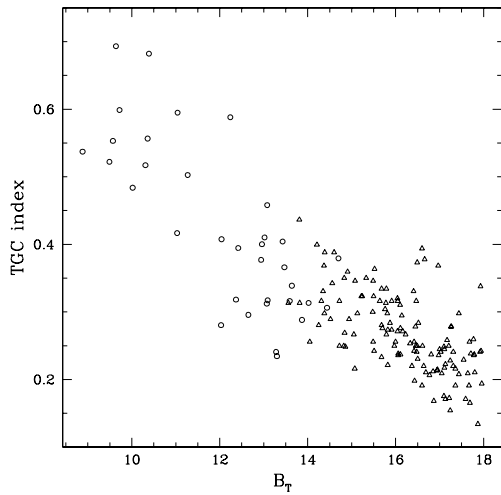


Fig. 8.— The TGC index is plotted against galaxy magnitude for a sample of Virgo dwarf Elliptical galaxies (triangles) taken from Jerjen, Binggeli, & Freeman (2000) and a sample of early-type Virgo and Fornax galaxies (circles) taken from Caon et al. (1993) and D’Onofrio et al. (1994). The TGC index has been derived using equation 7, and the magnitudes are the observed (i.e. not model-dependent) values. All galaxies which could be modelled with a Sérsic profile along the major-axis have been included.

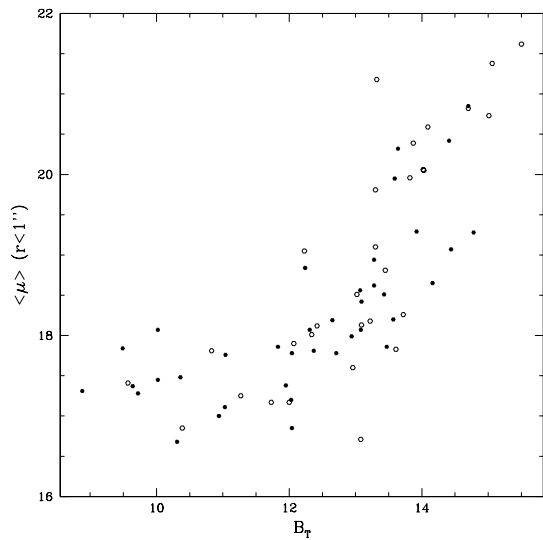


Fig. 9.— The observed (i.e. model-independent), central mean surface brightness within a circle of radius 1 arcsec is plotted against the observed (model-independent) galaxy magnitude. Filled circles represent Elliptical galaxies and open circles represent S0 galaxies from the complete Virgo and Fornax galaxy sample of Caon et al. (1993) and D’Onofrio et al. (1994) observed from the ground.

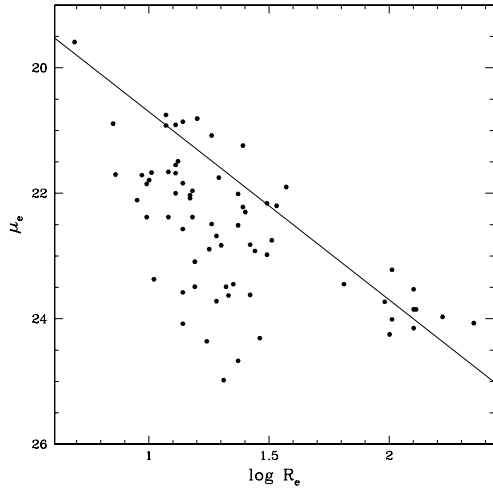


Fig. 10.— The (model-independent) surface brightness  $\mu_e$  at the (model-independent) effective half-light radius  $r_e$  is plotted against  $r_e$ . The data are from the complete Virgo and Fornax galaxy sample studied in Caon et al. (1993) and D’Onofrio et al. (1994).

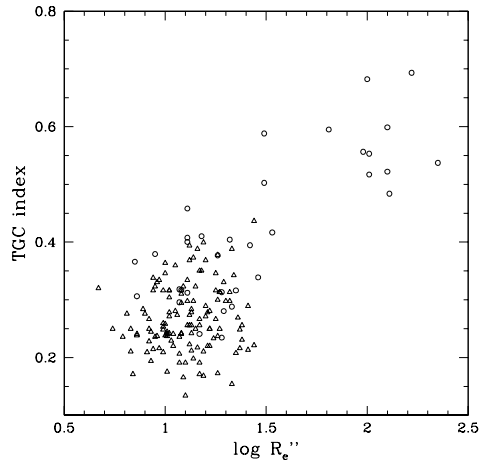


Fig. 11.— The TGC index shown in Figure 8 is plotted against each galaxy’s (model-independent) effective radii. Circles represent the early-type galaxies, and triangles represent the dwarf Elliptical galaxy sample.

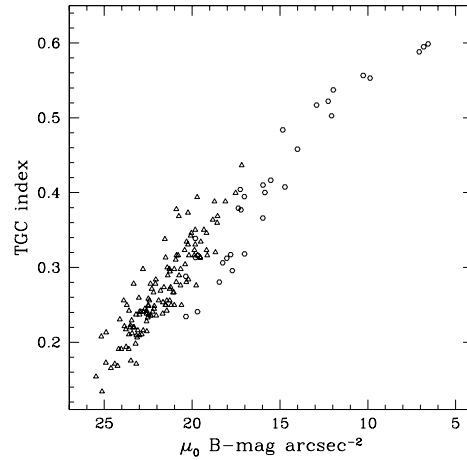


Fig. 12.— The TGC index shown in Figure 8 has been plotted against the central surface brightness of each galaxy. The only two galaxies with values for  $n$  greater than 10 have been excluded (see text for additional comments). Circles represent the early-type galaxies, and triangles represent the dwarf Elliptical galaxy sample.

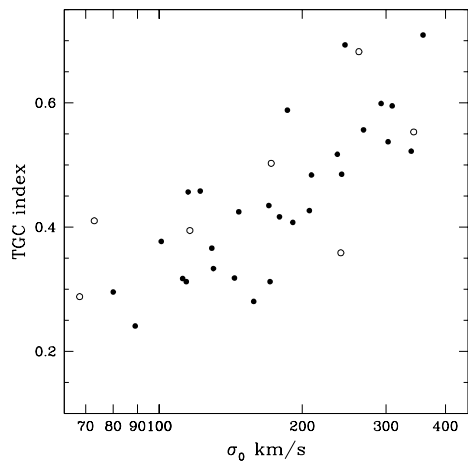


Fig. 13.— The TGC index shown in Figure 8 has been plotted against the central velocity dispersion for the early-type galaxies with published kinematical data. Filled circles represent the Elliptical galaxies, and open circles represent S0 galaxies.